Meteoritics 30, 294–302 (1995)

A petrographic history of martian meteorite ALH84001: Two shocks and an ancient age

ALLAN H. TREIMAN

Lunar and Planetary Institute, 3600 Bay Area Blvd., Houston, Texas 77058-1113, USA

(Received 1994 October 28; accepted in revised form 1995 January 21)

Abstract–ALH84001 is an igneous meteorite, an orthopyroxenite of martian origin. It contains petrographic evidence of two shock metamorphic events, separated by thermal and chemical events. The evidence for two shock events suggests that ALH84001 is ancient and perhaps a sample of the martian highlands. From petrography and mineral chemistry, the history of ALH84001 must include: crystallization from magma, a first shock (impact) metamorphism, thermal metamorphism, low-temperature chemical alteration, and a second shock (impact) metamorphism. Originally, ALH84001 was igneous, an orthopyroxene-chromite cumulate. In the first shock event, the igneous rock was cut by melt-breccia or cataclastic veinlets, now bands of equigranular fine-grained pyroxene and other minerals (crush zones). Intact fragments of the cumulate were fractured and strained (now converted to polygonized zones). The subsequent thermal metamorphism (possibly related to the first shock) annealed the melt-breccia or cataclastic veinlets to their present granoblastic texture and permitted chemical homogenization of all mineral species present. The temperature of metamorphism was at least 875 °C, based on mineral thermometers. Next, Mg-Fe-Ca carbonates and pyrite replaced plagioclase in both clasts and granular bands, producing ellipsoidal carbonate globules with sub-micron scale compositional stratigraphy, repeated identically in all globules. The second shock event produced microfault offsets of carbonate stratigraphy and other mineral contacts, radial fractures around chromite and maskelynite, and strain birefringence in pyroxene. Maskelynite could not have been preserved from the first shock event, because it would have crystallized back to plagioclase. The martian source area for ALH84001 must permit this complex, multiple impact history. Very few craters on young igneous surfaces are on or near earlier impact features. It is more likely that ALH84001 was ejected from an old igneous unit (Hesperian or Noachian age), pocked by numerous impact craters over its long exposure at the martian surface.

INTRODUCTION

The ALH84001 meteorite is an igneous rock, an orthopyroxene-chromite cumulate, which has been modified by shock, thermal metamorphism, and chemical alteration. It was originally classified as a diogenite. But recently it has been recognized as different from diogenites and originating on Mars (Mittlefehldt, 1994a), based principally on oxygen isotopes. ALH84001 is unique among martian meteorites; orthopyroxene-rich fragments are present in the other martian meteorites only as xenoliths in the EETA79001 basalt (Steele and Smith, 1982; McSween and Jarosewich, 1983). In addition, ALH84001 contains preterrestrial alteration materials of magnesite-siderite-ankerite carbonates and pyrite, an assemblage not identified in other martian meteorites (Gooding, 1992). So, ALH84001 is critically important in providing an additional view of igneous and chemical processes on Mars.

During examination of petrography of ALH84001, it became apparent that there was evidence for two distinct shock events, presumably meteorite impacts. None of the other martian samples shows evidence for multiple shock events, as could be expected from their young crystallization ages, ~180 Ma and 1.3 Ga (McSween, 1985; Jones, 1986). So, evidence for multiple shock events suggested that ALH84001 could be significantly older than the other martian meteorites, perhaps older than 3 Ga (Treiman, 1994a,b). Thus, ALH84001 may have come from an ancient martian surface (Hesperian or Noachian age), perhaps even from the martian highlands.

It may seem unusual to use petrography as a geochronologic tool. In this case, the petrography of ALH84001, in the context of martian geology and the cratering record of the inner Solar System, does imply a great age. This constraint, albeit imprecise, is valuable because ALH84001 will be difficult to date radiometrically. Age methods that rely on mineral isochrons are hampered because ALH84001 is almost monomineralic; K-Ar and Ar-Ar methods are hampered because of the potential for excess ^{40}Ar from the martian atmosphere (Swindle *et al.*, 1995) and the inhomogeneous distribution of K (bulk abundances of 108 ppm, Mittlefehldt, 1994b; 240 ppm, Dreibus *et al.*, 1994; 127 ± 6 ppm, Kallemeyn and Warren, pers. comm.). Methods that rely on acid leachates and residues (Jagoutz *et al.*, 1994) must assume that all minerals in ALH84001 are cogenetic and contemporaneous.

In this paper (building on Treiman, 1994a), I will present petrographic observations and mineral chemical data supplementing those of Mittlefehldt (1994a) and other workers to outline the geological history of ALH84001: igneous crystallization, first shock, thermal metamorphism, chemical alteration, and second shock. The inference of two separate shock events, separated in time by thermal metamorphism and low-temperature chemical alteration, is a significantly different from previously offered histories. The history of ALH84001 will then be used to derive constraints on its crystallization age and its possible martian sources.

PETROGRAPHY

ALH84001 is an orthopyroxenite, consisting of ~95% orthopyroxene, ~2% chromite, ~1% maskelynite, ~1% carbonate, and trace amounts of augite, apatite, olivine, and pyrite (Mittlefehldt, 1994a; Dreibus *et al.*, 1994; Harvey and McSween, 1994; Wadhwa and Crozaz, 1994). Augite is distinguishable from orthopyroxene by its greater birefringence but not by average atomic number (Z) in BSE imagery. ALH84001 contains two distinct petrographic domains, clasts and granular bands (Figs. 1–3; Figs. 1a,b of Mittlefehldt, 1994a), which are described below.

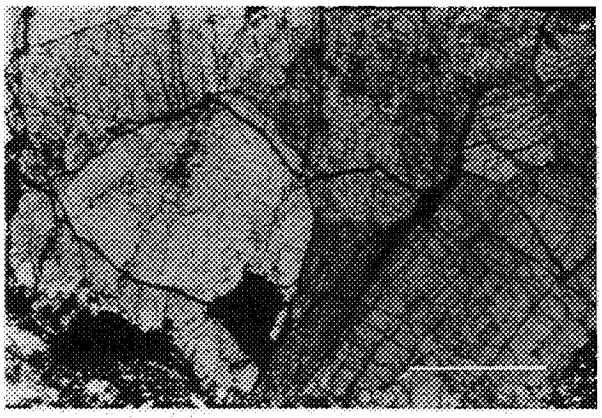

FIG. 1. Large coherent clast; crossed polarized light; scale bar = 1 mm. Grains in shades of gray are orthopyroxene; grains in black are chromite; small area of granular band to bottom corners. Note straight to slightly curving grain boundaries, abundant fractures, and strain birefringence in pyroxene.

Overall, the textures and structures in ALH84001 are comparable, but less cataclastic, than some lunar "recrystallized cataclastic rocks" (Stöffler *et al.*, 1980) or "metamorphic cataclastic rocks" (Ryder, 1982). Examples are 12073c, 15437 and 67955 (Ryder and Norman, 1979; Ryder, 1982; Taylor *et al.*, 1991).

Chemical analyses were obtained using the Cameca CAMEBAX electron microprobe at Johnson Space Center, NASA, Houston, Texas. Standards were well-characterized natural minerals and synthetic metals. Analyses were run at 15 kV accelerating voltage; beam current into a Faraday cup was 30 nA for pyroxenes and 10 nA for carbonates. Data were reduced with the ZAF routine (PAP) provided by Cameca. For carbonates, the ZAF routine automatically included 1 CO_2 per divalent cation equivalent.

Clasts

The clasts in ALH84001 are coherent fragments bounded by fine-grained granular bands. Clasts are up a few cm across and consist of orthopyroxene to 6 mm across, chromite to 2 mm across, and other grains to 0.5 mm across (Fig. 1; Berkley and Boynton, 1992; Mittlefehldt, 1994a). Mineral proportions in the clasts appear identical to those of the whole rock. In the clasts,

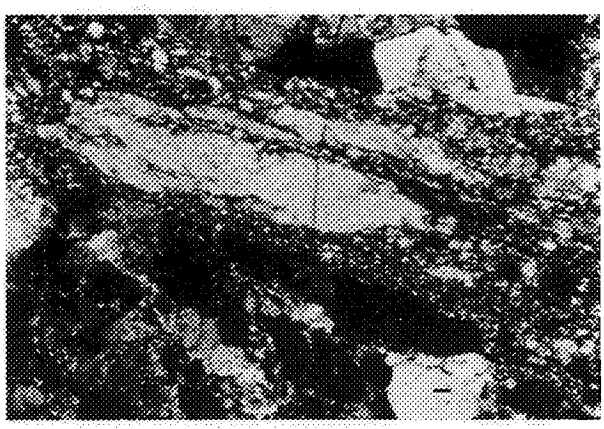

FIG. 2. Granular band (crush zone of Mittlefehldt, 1994a); crossed polarized light; scale bar = 100 μm. Flaser texture seen as elongated ribbons of orthopyroxene-rich rock in granular band.

FIG. 3. Granular band with showing chromite (black) drawn out into wavy stringer. Plane polarized light; scale bar = 100 μm. Elliptical carbonate globule (C) in clast within granular band.

orthopyroxenes are anhedral and without crystallographically controlled boundaries, except where they abut maskelynite. Pyroxene-pyroxene grain boundaries are straight to slightly curved. No exsolution features were noted in orthopyroxene (MacPherson, 1985). Chromite grains, equant and euhedral-subhedral, occur within and between orthopyroxenes. Augite, maskelynite, and apatite are restricted to angular regions interstitial to orthopyroxenes. The augite grains contain lamellar or lenticular structure visible as differences in refractive index and birefringence but not as atomic number (Z) contrast in BSE imagery. Carbonate and pyrite are concentrated in and near maskelynite. In maskelynite, carbonates form hemispherical to ellipsoidal globules with complex concentric zoning that is sharp on a sub-micron scale (Fig. 4; Fig. 1d of Mittlefehldt, 1994a). All carbonate globules in the clasts appear to have the same concentric sequence of layers and compositions: a central zone of ankerite, grading outward to ferroan magnesite (breunnerite) and thence to magnesite; an Fe-rich zone (bright in BSE imagery); a second magnesite zone; and a second Fe-rich zone (Fig. 4; Fig. 1 of Mittlefehldt, 1994a). Isolated

FIG. 4. Carbonate globules in a clast; backscattered electron image; scale bar = 100 μm Rounded globules of siderite-magnesite-ankerite solid solutions with intricate chemical zoning (bright = Fe-rich, dark = Mg-rich) replace plagioclase (P, now maskelynite, medium gray). Surrounding cracked light-gray grains are orthopyroxene; white grains are pyrite and chromite. Carbonate globule extends from maskelynite-rich interstitial area into granular band (larger arrows). Layering in carbonate globules transected by microfaults (smaller arrows).

patches of carbonate are present within orthopyroxene and along fractures. Pyrite occurs as discrete euhedra, ~10 μm across.

The clasts show many deformation features. The orthopyroxenes are extensively and pervasively cracked along cleavage directions (Fig. 1). Some cracks are wavy, and the grains and their cracks commonly are bent near granular bands. Orthopyroxene is commonly polygonized (converted to smaller grains), both where the fractures bend and along otherwise unmarked planes through the grains. Optical extinction in the pyroxenes is rarely sharp but is commonly irregular or undulose within grains. Microfaults in the clasts displace grain boundaries between silicate and oxide minerals (Fig. 1c of Mittlefehldt, 1994a) and displace layering in the carbonate globules (Fig. 4; Fig. 1d of Mittlefehldt, 1994a). Short fractures commonly radiate from chromite crystals and maskelynite patches in and among pyroxenes (Fig. 1a of Berkley and Boynton, 1992; Fig. 1c of Mittlefehldt, 1994a). Maskelynites contain a few fractures (Fig. 2).

Compositions of minerals in the clasts, except carbonates, are nearly homogeneous in major and trace-element compositions (Berkley and Boynton, 1992; Mittlefehldt, 1994a; Papike *et al.*, 1994; Harvey and McSween, 1994; Romanek *et al.*, 1994a,b; Wadhwa and Crozaz, 1994). Additional analyses of adjacent orthopyroxene and augite grains are given in Table 1. Carbonate compositions span a range from nearly pure magnesite, $Cc_4Mg_{95}Sd_1$, to magnesite-siderite solid solution, $Cc_{16}Mg_{48}Sd_{36}$, to ankeritic, $Cc_{25}Mg_{44}Sd_{31}$ (Mittlefehldt, 1994a; Romanek *et al.*, 1994a,b).

TABLE 1. Average compositions of adjacent augite and orthopyroxene in a clast.

	Augite 15 analyses	Orthopyroxene 8 analyses
SiO_2	53.72 ±0.44	54.41 ±0.20
TiO_2	0.30 ±0.04	0.18 ±0.03
Al_2O_3	0.56 ±0.22	0.56 ±0.06
Cr_2O_3	0.49 ±0.08	0.29 ±0.14
FeO	7.48 ±0.16	17.50 ±0.11
NiO	0.01 ±0.01	0.01 ±0.01
MnO	0.27 ± 0.02	0.51 ± 0.02
MgO	15.94 ± 0.21	25.59 ± 0.22
CaO	21.01 ± 0.41	1.52 ± 0.11
Na_2O	0.37 ± 0.03	0.02 ± 0.01
K_2O	0.01 ± 0.01	0.01 ± 0.005
Sum	100.16 ± 0.63	100.60 ± 0.31
Cations to 4 total		
Si	1.981 ± 0.005	1.975 ± 0.003
Ti	0.008 ± 0.001	0.005 ± 0.001
Al	0.024 ± 0.009	0.024 ± 0.002
Cr	0.014 ± 0.002	0.009 ± 0.004
Fe	0.231 ± 0.004	0.531 ± 0.004
Ni	0.000 ± 0.000	0.000 ± 0.000
Mn	0.009 ± 0.001	0.016 ± 0.001
Mg	0.876 ± 0.009	1.384 ± 0.009
Ca	0.830 ± 0.017	0.059 ± 0.004
Na	0.026 ± 0.002	0.002 ± 0.001
K	0.000 ± 0.000	0.000 ± 0.000
Molecular Endmembers		
Wo	42.5 ± 0.6	3.0 ± 0.2
En	45.2 ± 0.6	70.1 ± 0.3
Fs	11.9 ± 0.2	26.9 ± 0.2

Uncertainty shown is one standard deviation of population (1σ).

Granular Bands

ALH84001's clasts are separated by swaths (to a few mm wide) of fine-grained (10–30 μm diameter), granular textured orthopyroxene, chromite and maskelynite, apparently in the same proportions as the bulk rock (Figs. 2, 3). These swaths are called granular bands here and are the crush zones of Mittlefehldt (1994a). The granular bands consist of anhedral to subhedral orthopyroxene crystals (down to 10μm across) and anhedral chromite grains (20–0.1 μm across) with interstitial maskelynite and carbonates (Fig. 5). Many areas appear as unfoliated aggregates of even-sized grains (Fig. 1a, b of Mittlefehldt, 1994a), a granulitic texture in which pyroxene grains are commonly somewhat elongate along the cleavage direction but have random orientations and intergranular angles approaching 120° (decussate texture: Spry, 1969). In other areas, larger fragments (porphyroclasts) of orthopyroxenite sit in a fine-grained matrix, a classic "mortar" texture (Plate XXVIIIc of Spry, 1969). Some bands contain elongate fragments of clast orthopyroxenite (Fig. 2) in an augen or ribbon structure (Spry, 1969). Others contain wavy or swirled stringers of chromite (Fig. 3), sometimes continuous with (or traceable to) chromites in clasts. Texturally, the bands could be called recrystallized mylonite or pseudotachylite (Spry, 1969).

The granular bands show some of the deformation features of the clasts, notably cracks radiating from the larger chromite and maskelynite grains (Fig. 6; cracks displace orthopyroxene grains in

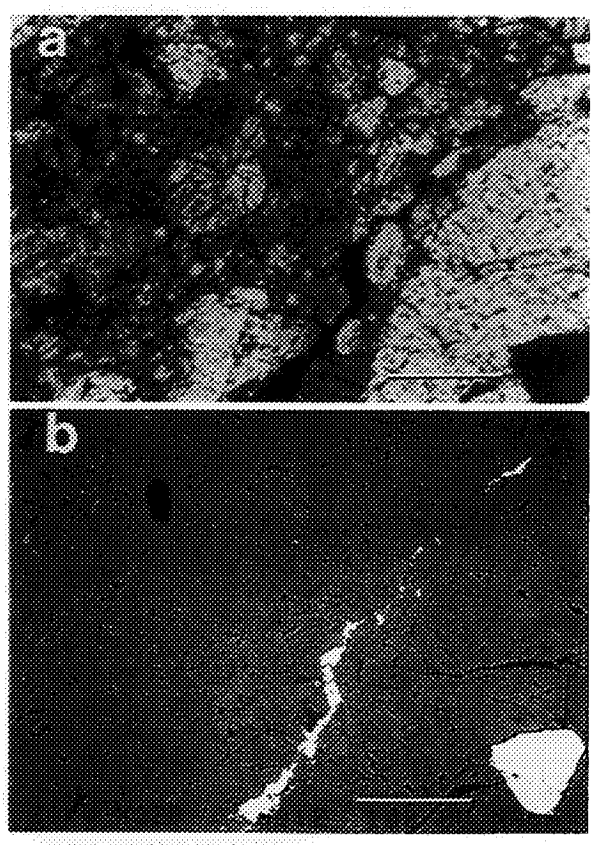

FIG. 5. Compact intergranular texture in granular band, on left, compared to clast texture, on right. Crossed-polarized light (5a) and back-scattered electron image (5b) of same area; scale bar =100 μm Mineral grains in granular band have a granulitic-polygonal texture (straight grain-boundaries, similar sized grains). There is no evidence of significant void space, broken fragments or irregular grain boundaries.

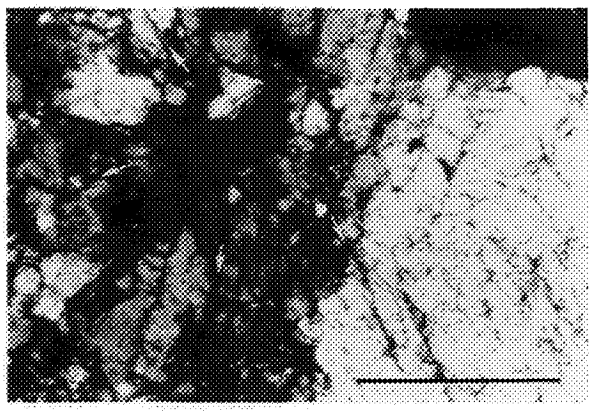

FIG. 6. Radial cracks around maskelynite in granular band; partially crossed polarized light; scale bar = 100 μm. Cracks cut and offset grains in granular band (arrows).

the granular band), and irregular or undulose optical extinction. However, the abundant cracks in the clasts do not extend into the granular bands but stop at the clast boundaries. Nor is polygonization observed, although it might not be apparent as the grain size of the granular bands is comparable to that formed by polygonization of clasts. Microfaults in the deformed bands are neither common nor obvious, but a few structures displace pyroxene and carbonate boundaries.

Carbonate is common in the granular bands but does not form coherent globules as in the clasts (Fig. 4). Rather, carbonate in the bands appears in thin section as patches of discrete grains among and between pyroxene grains; the patch of Fig. 7 is truly typical, not exemplary (it was chosen for photography and later study because of its proximity to the thin section edge). The carbonate-rich patches are not randomly dispersed in the granular bands, but they appear as circular to elliptical areas enriched in carbonate and lacking maskelynite. The microstratigraphy in the clast carbonate globules is repeated in these rounded patches, with each individual carbonate grain displaying a portion of the stratigraphic sequence. Stratigraphic marker horizons, like the bright layer of Fig. 7, can be traced from one carbonate grain to another, across intervening pyroxenes, to form "dashed circles." This suggests that carbonate grains in the granular bands are actually interconnected in three dimensions (outside the thin-section plane), and that the three-dimensional forms of the carbonate-rich areas are porous ellipsoidal globules. Essentially all carbonate in the granular bands is present in such round patches.

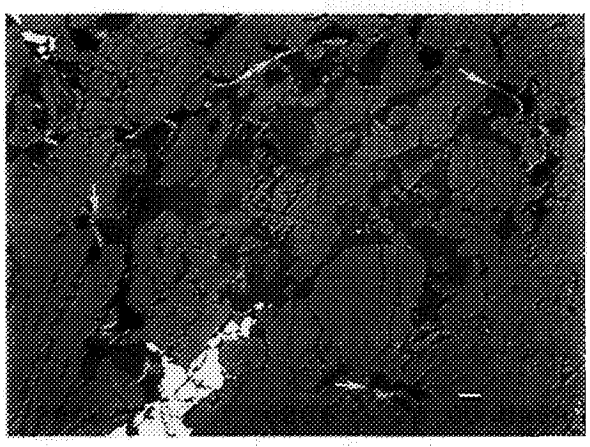

FIG. 7. Carbonate-rich patch in granular band; backscattered electron image; scale bar = 10 μm. Carbonate grades from light gray at center of globule (ankerite) through dark-gray or black (magnesite), with bright Fe-rich layers (arrows). Medium gray equant grains are pyroxene and white grains are chromite (*vis.*, Fig. 5). The Fe-rich bright layer (arrows) forms a "dashed circle," suggesting that the carbonate grains in the globule are physically continuous outside the section plane. As a whole, the carbonate patch shows a concentric stratigraphy identical to those of carbonates in clasts (Fig. 2), although piecewise in separated carbonate grains.

Compositions of minerals in the granular bands, except carbonates, are nearly homogeneous in major and trace-element compositions (Mittlefehldt, 1994a). Notably, chromites in the granular bands have a much more restricted compositional range than chromites in the clasts (Fig. 3 of Mittlefehldt, 1994a). Carbonate compositions in the granular bands span essentially the same range as in the clasts: nearly pure magnesite, $Cc_4Mg_{94}Sd_2$, to magnesite-siderite solid solution, $Cc_{15}Mg_{48}Sd_{37}$, to ankerite, $Cc_{42}Mg_{39}Sd_{19}$ (Table 2; Mittlefehldt, 1994a; Romanek *et al.*, 1994a,b).

GEOLOGICAL HISTORY

From these and literature data on ALH84001, the most significant events in its history were: crystallization from a magma, a first shock metamorphism, thermal metamorphism, low-temperature chemical alteration, and a second shock metamorphism. This history differs from that of Mittlefehldt (1994a) in having two shock events rather than one, and one alteration event at low temperature rather than two at high temperature. The most crucial observation here is that all the carbonate globules in ALH84001, in clasts or granular bands, are essentially identical in structure, internal stratigraphies, and compositions (Figs. 4, 7; Table 2; Figs. 1d and 5 of Mittlefehldt, 1994a). It seems highly unlikely that two distinct episodes of layering in the carbonate globules and their range of carbonate

TABLE 2. Extreme carbonate compositions in granular bands.

	Mg-richest	Fe-richest	Ca-richest
SiO_2	0.36	0.35	0.09
FeO	1.29	25.71	15.52
MnO	0.25	2.02	3.21
MgO	44.22	18.96	15.52
CaO	2.56	8.34	23.05
SO_3	0.05	0.03	0.03
CO_2*	51.25	44.26	45.32
Sum	99.98	99.68	100.75
Cations to 2 total			
Si	0.005	0.006	0.001
Fe	0.015	0.355	0.183
Mn	0.003	0.029	0.045
Mg	0.940	0.466	0.373
Ca	0.039	0.147	0.399
S	0.000	0.000	0.000
C	0.998	0.997	0.999
Molecular Endmembers			
Cc	3.9	15.2	41.8
Mg	94.5	48.2	39.1
Sd	1.6	36.6	19.1

* CO_2 calculated in 1:1 stoichiometry with atomic Fe + Mn + Mg + Ca.
Molecular endmembers are: CC, calcite, $CaCO_3$; Mg, magnesite, $MgCO_3$; and Sd, siderite, $CaCO_3$. Calculation ignores Mn, S, and Si.

alteration could yield such similar products. Further, the fine-scale compositions seem inconsistent with a high-temperature origin. If ALH84001 experienced one episode of alteration, it must have seen two shock events, because some of its shock effects are older than the alteration materials and some are younger. Features in ALH84001 attributable to the first (older) shock event include: the granular bands representing shock breccia or melt-breccia; pervasive cracking of pyroxene; and polygonized pyroxene, representing stress residual after the shock. Features attributable to the second (younger) shock event include: formation of maskelynite; microfault offsets cutting silicates, oxides, and carbonate globules; radial cracks around maskelynite and chromite; and stress represented as irregular extinction position in pyroxene.

Original Rock

Originally, ALH84001 was an igneous cumulate rock of orthopyroxene and chromite with interstitial plagioclase, augite, apatite, olivine, and possibly silica (Mittlefehldt, 1994a; Harvey and McSween, 1994; Fig. 1). This rock is now represented by the clasts as more-or-less disturbed fragments of an apparently homogeneous lithology. It is impossible to tell if mineral grains in the original (pre-shock) rock retained igneous zoning patterns, or had been chemically homogenized near to the level they are now: nearly constant compositions of orthopyroxene and chromite (Table 1; Mittlefehldt, 1994a). Compositions of maskelynite glass are more varied, which may reflect (in part) variations in the proportions of its parent phases (plagioclase + silica (+ alkali feldspar?); Mittlefehldt, 1994a). ALH84001 appears to be monomict, because all its clasts appear to be from the same orthopyroxene-chromite cumulate, and there is no evidence that the granular bands contain any material besides that represented by the clasts.

First Shock Metamorphism

ALH84001 is criss-crossed by granular bands (crush zones of Mittlefehldt, 1994a), which are interpreted as products of a shock metamorphism, presumably from a meteorite impact (Fig. 1a,b and text of Mittlefehldt, 1994a). The structures of the granular bands are typical of dynamic metamorphism (high strain rates), which can occur during rapid tectonic motions or during shock (Spry, 1969). Characteristic structures of dynamic metamorphism include fragments of host rock (clasts) in a fine-grained matrix of the same material (Figs. 1, 2; Fig. 1a of Mittlefehldt, 1994a), ribbon structures (Fig. 2), and fluidal structures (swirling strings of chromite grains, Fig. 3). From ALH84001 alone, it is difficult to determine whether this dynamic metamorphism reflects tectonics or shock, although the random orientations of the granular bands suggest going against a tectonic origin (Fig. 1a of Mittlefehldt, 1994a). From the perspective of a martian origin, shock is far more likely than tectonic deformation (abundances of impact craters *vs.* tectonic features; Tanaka *et al.*, 1992; Branerdt *et al.*, 1992; Schulz and Tanaka, 1994), and I infer that this metamorphism reflects shock from a meteorite impact.

The granular bands were likely to have been melt-breccia dikelets originally, although they might have been crystalline cataclasites. Melt-breccias, fragmental breccias with glassy matrices, are common in highly shocked materials, stages S5 and S6 of Stöffler *et al.* (1991). A melt-breccia origin is consistent with limited differential movement within and across granular bands, and with the wavy and swirly stringers of chromite (Fig, 3); similar wavy structure in a melt-breccia dike (albeit not in chromite but in opaque shock-melt) is shown in Fig. 17 of Stöffler *et al.* (1991). If the granular bands had been wholly molten, they would probably show remnants of crystals grown from the melt, like the dendritic olivine and pyroxene crystals in shock-melt dikelets in ALHA77005 and LEW88516 (Treiman *et al.*, 1994). If the bands had been wholly crystalline, like fault gouge, it is not obvious that the wavy and swirly stringers of chromite could have been produced or preserved.

Other deformation features attributable to this first shock event are pervasive cracking along cleavage of the clast pyroxenes, deformation of those cracks from straight to wavy, bending of the cracks at the edges of granular bands, and probably intracrystalline stress that was relieved to form the polygonized areas and planes.

There is no evidence one way or the other that the shock event affected the compositions of ALH84001 and its constituent minerals. As noted above, the granular bands have the same mineralogy, mineral proportions, and (for the most part) mineral compositions as the clasts. The extreme homogeneity of chromite compositions in the granular bands (compared to those in clasts) could be ascribed to high temperature during their formation. It could also be ascribed to the subsequent thermal event and the small grain size in the granular bands.

In this first impact event, ALH84001 was not likely to have been part of the ejecta. More likely, it remained part of the shocked basement rock. Ejecta breccias and intracrater breccias are usually polymict, containing clasts that are compositionally distinct from the breccia matrix, or containing a variety of clasts (Stöffler *et al.*, 1980; Hörz *et al.*, 1991). However, ALH84001 is likely monomict, as minerals in the granular bands and their proportions are identical to those of the clasts, suggesting that this shock event introduced little or no exogenous material. Monomict breccias, structurally comparable to ALH84001, are usually interpreted as forming in the bedrock beneath an impact crater (Hörz *et al.*, 1991). It seems reasonable to infer a similar origin for ALH84001.

Thermal Metamorphism: Textural Annealing and Chemical Equilibration

After the first shock, ALH84001 experienced thermal metamorphism of sufficient temperature and time to anneal the granular bands to their current granoblastic-polygonal texture (Fig, 5). The nearly homogeneous mineral compositions throughout the rock may have been a result of this event or may reflect post-igneous cooling. However, compositions of chromites in the granular bands are even more restricted than in the clasts (Mittlefehldt, 1994a), which might suggest speedier chemical equilibration among bands' small mineral grains. Only the alteration mineral assemblage, carbonates + pyrite, was unaffected by thermal metamorphism.

Thermal metamorphism is required to explain intergranular textures within the granular bands. If the bands are correctly interpreted as originally being cataclastic or melt-breccia zones, they would have had textures including broken angular grains, irregular grain boundaries, possibly inter-grain void spaces, and glass. However, the granular bands now consist of larger fragments in a granoblastic polygonal matrix, as shown in Fig. 5. The matrix grains are not irregular or broken, no void spaces are present, and there is no glass (save maskelynite after plagioclase). This inferred transformation from cataclastic or melt breccia textured pyroxenite to granoblastic polygonal textured pyroxenite would seem to

require the time-at-high-temperature of a metamorphic event. The ALH84001 clasts might show little textural evidence of this metamorphism, as their textures resumably already reflected the high temperatures of igneous crystallization and post-igneous cooling.

The maximum metamorphic temperature was at least 875 °C, as given by mineral geothermometers. The composition of augite adjacent to orthopyroxene (Table 1) yields an equilibration temperature of 875 °C using the Davidson and Lindsley (1985) two-pyroxene thermometer. No correction to their calibration is needed as the ALH84001 augite contains almost no non-quad components. The Fe-Mg distribution between ALH84001 olivine (34.5% Fa; Harvey and McSween, 1994) and augite (Table 1) suggest equilibration at 1040 ± 180 °C (Kawasaki and Ito, 1994); Fe-Mg distribution between olivine and orthopyroxene of these compositions is not sensitive to temperature (von Seckendorf and O'Neill, 1993). Fe-Mg distribution between ALH84001 chromite and olivine (Mittlefehldt, 1994a; Harvey and McSween, 1994) suggests equilibration at ~900 °C (Sack and Ghiorso, 1991). The Fe-Mg distribution between chromite and orthopyroxene yields equilibration temperatures of 635–710 °C (depending on chromite composition used) following the calibration of Mukherjee *et al.* (1990). Mittlefehldt (1994c) noted that this calibration gave temperatures 0–200 °C below two-pyroxene temperatures. All of these geothermometers give "closure" temperatures for chemical equilibration among their minerals, not peak metamorphic temperatures. The peak temperature experienced by ALH84001 could have been much higher, but its chemical signature would have been erased by equilibration to the closure temperature.

Mittlefehldt (1994a) inferred a higher equilibration temperature, ~1050 °C, using orthopyroxene composition alone in the two-pyroxene thermometer of Lindsley and Anderson (1983). This temperature is quite uncertain because the composition of orthopyroxene in equilibrium with augite changes little with changing temperature (Fig. 6 of Lindsley and Anderson, 1983); thus, small inaccuracies in composition, location of the pyroxene miscibility gap, estimation of ferric iron content, or correction for non-quad pyroxene components can shift apparent equilibrium temperatures by hundreds of degrees. Compositions of augite in equilibrium with orthopyroxene change much more rapidly with temperature, and so yield much more precise temperatures. The augite of Table 1 suggests equilibration at ~850 °C in the Lindsley and Andersen (1983) thermometer, compared to 875 °C in the formulation of Davidson and Lindsley (1985). Davidson and Lindsley (1985) noted that their thermometer tended to give temperatures ~25 °C higher than the Lindsley and Anderson (1983) thermometer.

The thermal metamorphism may have been part of the first shock metamorphism; heat generated by a meteorite impact dissipated slowly enough to permit extensive chemical equilibration. Or, the thermal metamorphism might have been a separate event, such as a later impact or a nearby igneous intrusion. In any case, the thermal metamorphism was dry, because ALH84001 contains no hydrous minerals (*e.g.,* amphibole, chlorite) that might have formed during cooling (retrograde metamorphism) in a water-rich environment.

Alteration

After thermal metamorphism, ALH84001 experienced a single episode of low-temperature chemical alteration in which plagioclase (silica) throughout the rock was partially replaced by Mg-Fe-Ca carbonates in globular concentric structures (Figs. 4, 7; Fig. 1d of Mittlefehldt, 1994a). No silicate alteration phases or hydrous non-silicates have been recognized. Mittlefehldt (1994a) inferred that ALH84001 experienced two episodes of alteration at high temperature: early alteration represented by the strongly zoned carbonate globules in the clasts; and late alteration represented by carbonates in the granular bands. But petrographic and chemical evidence suggests that the alteration of ALH84001 can be ascribed to a single episode, after thermal metamorphism, and at low temperature.

The similarity and near-identity of carbonate-rich globules in granular bands and in clasts suggests that all formed in a single episode. Carbonates in clasts and in granular bands both occur in ellipsoidal shapes, "globules" or "patches" (Figs. 4, 7). The compositions of carbonates in clasts and in granular bands have essentially identical ranges ($Cc_4Mg_{95}Sd_1$, $Cc_{16}Mg_{48}Sd_{36}$, $Cc_{25}Mg_{44}Sd_{31}$ and $Cc_4Mg_{94}Sd_2$, $Cc_{15}Mg_{48}Sd_{37}$, $Cc_{42}Mg_{39}Sd_{19}$ respectively; Table 2; Mittlefehldt, 1994a; Romanek *et al*, 1994a). Carbonates in clasts and in granular bands both have identical concentric layering, or stratigraphy (*e.g.,* Figs. 4, 7). Carbonate in the granular bands is essentially all associated with these rounded patches, suggesting that little if any carbonate was present before formation of the granular bands. Some carbonate globules straddle boundaries between clasts and granular bands, with stratigraphic layers traceable from clast into granular band (Fig. 4). So, a single episode of alteration is sufficient to explain the carbonates in ALH84001; no available evidence requires two episodes. Invoking Occam's razor, I will proceed assuming a single episode of aqueous alteration.

The carbonate must have been deposited after the granular bands had annealed, because the concentric stratigraphy of the carbonate globules is superimposed on the equilibrated granular texture of the bands (Fig. 7). Since all the carbonate in ALH84001 formed in a single episode (see above), that episode post-dated annealing, and therefore the thermal metamorphism described above. Deformation structures that cut the carbonate globules can be ascribed to a second shock metamorphism, see below.

Finally, the stratigraphy and compositions of the carbonate globules suggest that they formed at low temperature, not high temperature as suggested by Mittlefehldt (1994a) and Harvey and McSween (1994). The sub-micron scale chemical zoning visible in the clast carbonates (Fig. 4; Fig. 1d of Mittlefehldt, 1994a) could not have persisted at high or sub-magmatic temperatures (~700 °C: Mittlefehldt, 1994a; ~550° C: Harvey and McSween, 1994). For instance, experiments involving submicron grains of Fe-Mg carbonates in flux effectively homogenize in days at 500 °C and in a month at 350 °C (Rosenberg, 1963, 1967). Clearly, the ALH84001 carbonates did not experience such high temperatures as they are strongly zoned (Figs. 4, 7; Table 2; Figs. 1d, 5 of Mittlefehldt, 1994a). Comparable chemical heterogeneity is preserved in low-temperature carbonates on Earth (*e.g.,* Mozely, 1989). The actual temperature of carbonate formation is poorly constrained, with lower temperature estimates ranging from 0 to 320 °C (Grady *et al.*, 1994; Romanek *et al.*, 1994a,b). All but the lowest temperatures in this range seem to be inconsistent with the absence of silicate alteration minerals like chlorite and clays (*e.g.*, Gooding, 1986; Gislason *et al.*, 1993; Noack *et al.*, 1993). However, the presence of magnesite rather than the hydrous Mg carbonates nesquehonite [$Mg(HCO_3)(OH)\cdot 2H_2O$] and hydro-

McSween H. Y., Jr. and Jarosewich E. (1983) Petrogenesis of the Elephant Moraine A79001 meteorite: Multiple magma pulses on the shergottite parent planet. *Geochim. Cosmochim. Acta* **47,** 1501–1513.

Melosh H. J. (1989) *Impact Cratering: A Geologic Process.* Oxford Univ. Press, New York.

Mittlefehldt D. W. (1994a) ALH84001, a cumulate orthopyroxenite member of the SNC meteorite group. *Meteoritics* **29,** 214–221.

Mittlefehldt D. W. (1994b) Erratum to "ALH84001, a cumulate orthopyroxenite member of the SNC meteorite group." *Meteoritics* **29,** 900.

Mittlefehldt D. W. (1994c) The genesis of diogenites and HED parent body processes. *Geochim. Cosmochim. Acta* **58,** 1537–1552.

Mouginis-Mark P. J., McCoy T. J., Taylor G. J. and Keil K. (1992) Martian parent craters for the SNC meteorites. *J. Geophys. Res.* **97,** 10,213–10,226.

Mozley P. S. (1989) Relationship between depositional environment and the elemental composition of early diagenetic siderite. *Geology* **17,** 704–706.

Mukherjee A. B., Bulatov V. and Kotelnikov A. (1990) New high P-T experimental results on orthopyroxene-chrome spinel equilibrium and a revised orthopyroxene-spinel cosmothermometer. *Proc. Lunar Planet. Sci. Conf.* **20th,** 299–308.

Nishiizumi K., Caffee M. W. and Finkel R. C. (1994) Exposure histories of ALH 84001 and ALHA 77005 (abstract). *Meteoritics* **29,** 511.

Noack Y., Colin F., Nahon D., DelVigne J. and Michaux L. (1993) Secondary-mineral formation during natural weathering of pyroxene: Review and thermodynamic approach. *Am. J. Sci.* **293,** 111–134.

Papike J. J., Fowler G. W., Layne G. D., Spilde M. N. and Shearer C. K. (1994) ALH 84001 a "SNC orthopyroxenite": Insights from SIMS analysis of orthopyroxene and comparison to diogenites (abstract). *Lunar Planet. Sci.* **25,** 1043–1044.

Romanek C. S., Mittlefehldt D. W., Gibson E. K., Jr. and Socki R. A. (1994a) Martian carbonates in ALH84001: Textural, elemental, and stable isotopic compositional evidence on their formation (abstract). *Meteoritics* **29,** 523.

Romanek C. S., Grady M. M., Wright I. P., Mittlefehldt D. W., Socki R. A., Pillinger C. T. and Gibson E. K., Jr. (1994b) Record of fluid-rock interactions on Mars from the meteorite ALH 84001. *Nature* **372** 655–657.

Rosenberg P .E. (1963) Synthetic solid solutions in the systems $MgCO_3$-$FeCO_3$ and $MnCO_3$-$FeCO_3$. *Amer. Mineral.* **48,** 1396–1400.

Rosenberg P. E. (1967) Subsolidus relations in the system $CaCO_3$-$MgCO_3$-$FeCO_3$ between 350 and 550 °C. *Amer. Mineral.* **52,** 787–797.

Ryder G. (1982) Nutshell guide to lunar breccias. In *Workshop on Lunar Breccias and Soils and their Meteoritic Analogs* (eds G. J. Taylor and L. L. Wilkening), p. 111–119. L.P.I. Tech. Rept. 82-02. Lunar and Planetary Institute, Houston, Texas.

Ryder G. and Norman M. (1979) *Catalog of Pristine Non-Mare Materials Part I. Non-Anorthosites Revised.* JSC-14565, Johnson Space Center, Houston, Texas.

Sack R. O. and Ghiorso M. S. (1991) Chromian spinels as petrogenetic indicators: Thermodynamics and petrological applications. *Amer. Mineral.* **76,** 827–847.

Schulz R. A. and Tanaka K. L. (1994) Lithosphere-scale buckling and thrust structures on Mars: The Coprates rise and south Tharsis ridge belt. *J. Geophys. Res.* **99,** 8371–8385.

Spry A. (1969) *Metamorphic Texture.* Pergamon Press, New York. 350 pp.

Steele I. M. and Smith J. V. (1982) Petrography and mineralogy of two basalts and olivine-pyroxene-spinel fragments in achondrite EETA79001. *Proc. Lunar Planet. Sci. Conf.* **13th,** *J. Geophys. Res.* **87** (suppl.), A375–A384.

Stöffler D., Knöll H.-D., Marvin U. B., Simonds C. H. and Warren P. H. (1980) Recommended classification and nomenclature of lunar highland rocks—a committee report. In *Proceedings of the Conference on the Lunar Highlands Crust* (eds. J. J. Papike and R. B. Merrill), pp. 51–70. Pergamon Press, New York.

Stöffler D., Ostertag R., Jammes C., Pfannschmidt G., Sen Gupta P. R., Simon S. B., Papike J. J. and Beuachamp R. H. (1986) Shock metamorphism and petrography of the Shergotty achondrite. *Geochim. Cosmochim. Acta* **50,** 889–913.

Stöffler D., Keil K. and Scott E. R. D. (1991) Shock metamorphism of ordinary chondrites. *Geochim. Cosmochim. Acta* **55,** 3845–3867.

Swindle T. D., Grier J. A. and Burkland M. K. (1995) Noble gases in orthopyroxenite ALH84001: A different kind of martian meteorite with an atmospheric signature? *Geochim. Cosmochim. Acta* **59,** in press.

Tanaka K., Scott D. H. and Greeley R. (1992) Global Stratigraphy. In *Mars* (eds. H. Kieffer, B .M. Jakosky, C. W. Snyder and M. S. Matthews), pp. 345–382. Univ. Arizona Press, Tucson, Arizona.

Taylor G. T., Warren P., Ryder G., Delano J., Pieters C. and Lofgren G. (1991) Lunar rocks. In *Lunar Sourcebook: A Users Guide to the Moon* (eds. G. H. Hieken, G. T. Vaniman and B. M. French), pp. 183–284. Cambridge Univ. Press, New York, New York.

Treiman A. H. (1994a) An ancient age for ALH84001? Petrographic evidence for multiple shock events (abstract). *Meteoritics* **29,** 542.

Treiman A. H.(1994b) SNC: Multiple source areas for martian meteorites. *J. Geophys. Res.* **100,** in press.

Treiman A. H., Drake M. J., Janssens M.-J., Wolf R. and Ebihara M. (1986) Core formation in the Earth and the Shergottite Parent Body (SPB): Chemical evidence from basalts. *Geochim. Cosmochim. Acta* **50,** 1071–1091.

Treiman A. H., Barrett R. A. and Gooding J. L. (1993) Preterrestrial aqueous alteration of the Lafayette (SNC) meteorite. *Meteoritics* **28,** 86–97.

Treiman A. H., McKay G. A., Bogard D. D., Mittlefehldt D. W., Wang M.-S., Keller L., Lipschutz M. E., Lindstrom M. M. and Garrison D. (1994) Comparison of the LEW88516 and ALHA77005 martian meteorites: Similar but distinct. *Meteoritics* **29,** 581–592.

von der Borch C. (1965) The distribution and preliminary geochemistry of modern carbonate sediments of the Coorong area, South Australia. *Geochim. Cosmochim. Acta* **29,** 781–799.

von Seckendorf V. and O'Neill H. St. C. (1993) An experimental study of Fe-Mg partitioning between olivine and orthopyroxene at 1173, 1273, and 1423 K and 1.6 GPa. *Contrib. Mineral. Petrol.* **113,** 196–207.

Wadhwa M. and Crozaz G. (1994) First evidence for infiltration metasomatism in a martian meteorite: ALH84001 (abstract). *Meteoritics* **29,** 545.

Warren P. H. (1994) Lunar and martian delivery services. *Icarus* **111,** 338–363.

Wilhelms D. E. and Baldwin R. J. (1989) The role of igneous sills in shaping the martian uplands. *Proc. Lunar Planet. Sci. Conf.* **19th,** 355–365.